# Experimental modal analysis of emergency shelters in Montréal, Canada

**F. Mirshafiei & G. McClure**
*Civil Engineering and Applied Mechanics, McGill University*

**SUMMARY:**
Two popular nondestructive methods to assess the dynamic properties of building structures are ambient vibration and forced vibration experiments. Ambient vibration testing offers an important advantage over forced vibration techniques as it does not require any special excitation of the structure. Massive structures may indeed require strong forced excitation levels that are not always possible in operational buildings, and floor system alterations are typically required to restrain the shaker, which is also constraining.

This paper presents the operational modal analysis results of a series of ambient vibration tests performed on low and mid-rise buildings designated as emergency shelters in Montréal, Canada. Fundamental mode shapes, modal frequencies and corresponding modal damping ratios were determined from the records, based on advanced frequency domain decomposition techniques available in commercial software. The modal identification is an important step in the validation of finite element analysis models, assessment of current structures and health monitoring purposes.

*Keywords: Earthquake engineering, ambient vibration tests, modal characteristics, low-rise buildings.*

## 1. INTRODUCTION

When a building is subjected to dynamic loads, its structural response depends on the frequency content and magnitude of the forces exciting the structural system, the dynamic properties of the building (natural frequencies, mode shapes and damping ratios), the variation of these parameters in time if the building behaves nonlinearly during strong motions, as well as the soil type and foundation underneath of the superstructure. Therefore, the first step to predict the dynamic response of a structure is to estimate its natural or operational dynamic characteristics. However, it is important to acknowledge the difference between the dynamic response measured *in situ* and the response predicted by an idealized computational model under selected loading scenarios. Therefore, to help calibrate computational building models, and get more realistic results and improved understanding of their dynamic properties, three different categories of *in situ* tests have been developed through the last century (see a review in Hans, Boutin et al. 2005) :

1) Ambient vibration test (AVT): Owing to technological advances in sensing techniques, this method has received more attention from the 1990s and has been the most popular method for testing real structures in recent years. AVT is of easy application in large structures, low cost and its results are reliable. High resolution sensors are available at relatively low cost (for engineering studies), which can measure ambient horizontal accelerations of the order of $10^{-5}g$ at the base level to $10^{-4}g$ at the top of the buildings.
2) Harmonic forcing (shaker): a harmonic shaker with controlled forcing frequency is used to identify the resonant natural frequencies of the structure. A typical device usually induces a horizontal acceleration of the order of $10^{-4}g$ at the building base and $10^{-3}g$ at the top, which is about 10 times greater ambient levels.

3) Shocks: Shock testing on buildings is performed by impacting the upper part of the structure separately along the two principal axes by means of a heavy mechanical shovel (impactor). This shock loading induces transient accelerations that are about a thousand times greater than the ambient level.

In all these tests, the accelerations are small enough to keep the structure within its elastic range of response. Several authors (Trifunac 1972; Lamarche, Paultre et al. 2008), have shown that forced and ambient tests will lead to consistent agreement of modal parameters of the building structure. Hans *et al*. (2005) also showed with three building test campaigns that all three techniques yielded almost to the same results. Their study also confirmed that building natural frequencies tend to decrease while the vibration amplitude increases (from ambient to shock load), but this reduction was observed to be very small, about only 2 to 5% while the excitation amplitude had been increased by $10^3$.The same trend has also been observed by other researchers: the reliability of AVT in real structures has been proved and such techniques have been used worldwide for updating finite element models (Venture, Brincker et al. 2001; Yu, Taciroglu et al. 2007; Yu, Taciroglu et al. 2007; R. Tremblay 2008; Charles-Philippe Lamarche, Proulx et al. 2009), detecting changes in dynamic behavior of structures after retrofitting or damage, structural identification and predicting the seismic behavior of buildings (Gilles 2011; Gentile and Gallino 2008; Michel, Guéguen et al. 2008).

This paper presents results extracted from ambient vibration tests performed on three emergency shelters in Montréal. In total, nine buildings were tested and details of measurements, building characteristics and mode shapes are presented next. These are low and mid-rise buildings with both plan and vertical irregularities, thus exhibiting coupled sway and torsional modes in the low frequency range.

## 2. AMBIENT VIBRATION TESTING PROCEDURE

### 2.1 AVT set up and protocol

In the study, seven Tromino™ wireless sensors (tromographs – see www.tromino.eu) are used to record horizontal and vertical accelerations and velocities of building roof/floors. A typical set up of the instrument is shown in Fig. 2.1: it comprises the sensor itself (small red box) and a radio antenna amplifier which allows the network of sensors to communicate. The system is completely wireless and the data is recorded directly in the sensor for eventual download to a computer using a standard USB connection.

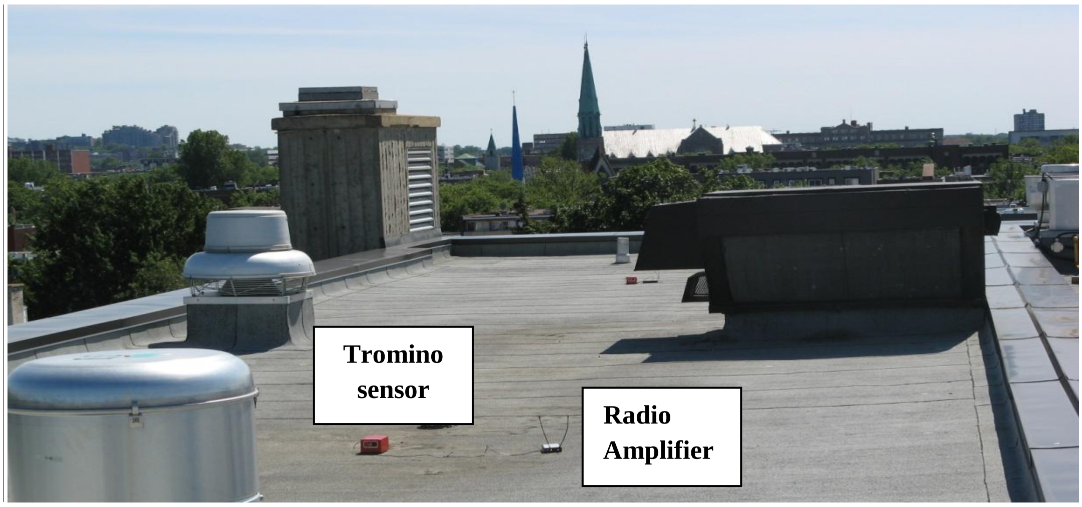


**Figure 2.1**. One Tromino™ sensor and its radio antenna amplifier

For each building, velocities resulting from ambient excitations (such as wind, traffic outside the building, normal building operations and human activities) are measured at least in three different locations on all floors, typically one near the center and the other two far away from the center, along a principal axis of rigidity or a main geometric axis. Each sensor records velocities and accelerations in three orthogonal directions: two in the horizontal plane and one in the vertical direction. Moreover, as the study deals with low rise buildings, some of them could have flexible roofs and in such cases, more sensors are deployed on the roof to capture this effect. Two sensors (instead of only one) are designated as reference and are deployed on the top floors and far from the center of rigidity. In general, ten-minute data records were taken at a sampling frequency of 128 Hz. Since only building frequencies below 20 Hz are of interest, the recorded data were decimated in order of three to reduce noise.

## 2.2. Estimation of modal parameters

In this study, ARTeMIS™ software (Solution, S.V. 2010) Handy Extractor version is used to treat the recorded data. Two methods are available, Frequency Domain Decomposition (FDD) and Enhanced Frequency Domain Decomposition (EFDD), to extract the lower frequency modal parameters of the buildings.  The results obtained from both methods are compared, and the final modal characteristic estimates reported in this paper are based on the authors' view.

An important step in any frequency domain system identification method is to calculate power spectral densities (PSD) of recorded data. Spectral density is a direct measure of a signal's energy content per unit frequency. Therefore, it is a useful mathematical tool to identify frequencies that contribute the most energy to a particular signal: if the input signal is a white noise, then the peaks of the output PSD function correspond to the natural frequencies of the system. The first step of Frequency Domain Decomposition (FDD) method is to estimate the spectral densities between all the recorded data channels to assemble the PSD matrix, $G_{xy}(\omega)$. The PSD is defined as the expected value of the product of Fourier transforms of all pairs of recorded data. However, as indicated in Equation (2.1), the PSD is estimated by dividing each signal into n sub-records of shorter duration and, omitting the expected value operation, and averaging the multiplication of corresponding pairs of discrete Fourier transforms.

$$G_{xy}(\omega) \approx \frac{1}{n}\sum_{a=1}^{n} X^{a}(\omega)Y^{a}(\omega)^{*} \tag{2.1}$$

where * denotes the complex conjugate, $X(\omega)$ and $Y(\omega)$ are the discrete Fourier transforms of corresponding time history records and n is the number of sub records.

It is possible to estimate resonant natural frequencies by the classical frequency domain method called peak-picking, which involves plotting each spectral density function by considering one element of the PSD matrix over the frequency range of interest, and identifying the peaks as natural frequencies. However, this classical method has difficulties to identify closely-spaced modes. Therefore, two other more sophisticated methods (FDD and EFDD) have been used in the study to overcome this problem. The two methods are briefly presented next.

### *2.2.1 Frequency Domain Decomposition (FDD)*

FDD is consisted of decomposing the PSD matrix into its eigenproblem form by singular value decomposition as follows:

$$G\ (\omega) = [U(\omega)][S(\omega)][U(\omega)]^{H} \tag{2.2}$$

Where H means Hermitian transformation, [U] is unitary matrix (containing the singular vectors), [S] is the matrix of singular values and G is the power spectral density matrix. The singular vectors represent the system mode shapes and the corresponding singular values provide an estimate of the contribution of each mode to overall energy at each frequency. In fact, the singular value decomposition of the output PSD matrix is an approximation to its modal decomposition (Brincker, Zhang et al. 2001). Resonant frequencies are identified from the peaks on the first singular value plot, and at each resonant frequency, the first singular vector provides an estimate of the associated mode shape.

*2.2.2 Enhanced Frequency Domain Decomposition (EFDD)*
EFDD adds a modal estimation layer to the FDD peak-picking. It proceeds in two steps: the first step is to perform FDD peak picking as described above, and the second step is to use the FDD-identified mode shape to construct a single-degree-of-freedom (SDOF) spectral bell function which is used to estimate the natural frequency and damping ratio for the mode. The construction of the SDOF spectral bell is performed using the FDD identified mode shape as reference vector and proceeds with a correlation analysis based on a modal assurance criterion (MAC) (see Equation 2.3). MAC values are calculated between the reference vector and the other singular vectors (on each side of the FDD-identified frequency). If the largest MAC value of these vectors exceeds a user-specified MAC Rejection Level (set to 0.8 in the study) then the corresponding singular values are included in the description of the SDOF Spectral Bell.

$$MAC(\{\varphi_1\},\{\varphi_2\}) = \frac{\left|\{\varphi_1\}^H.\{\varphi_2\}\right|^2}{\left|\{\varphi_1\}^H.\{\varphi_1\}\right|.\left|\{\varphi_2\}^H.\{\varphi_2\}\right|} \tag{2.3}$$

The natural frequency and damping ratio are computed by transferring the SDOF spectral bell to time domain. This time function is similar to the auto correlation function of the velocity of a linear SDOF oscillator subjected to white noise excitation, and it is straightforward to determine the function frequency and equivalent viscous damping ratio by simple linear regression. (Brincker, Ventura *et al.* 2001).

## 3. MODE SHAPES OF THE TESTED SHELTERS

### 3.1 Complex A: *Patro Le Prévost*

This complex constructed in 1975 and comprising five joint-separated buildings is illustrated in Figure 3.1. The north direction is an assumed reference that will be used for consistency in the orientation of all sensors.

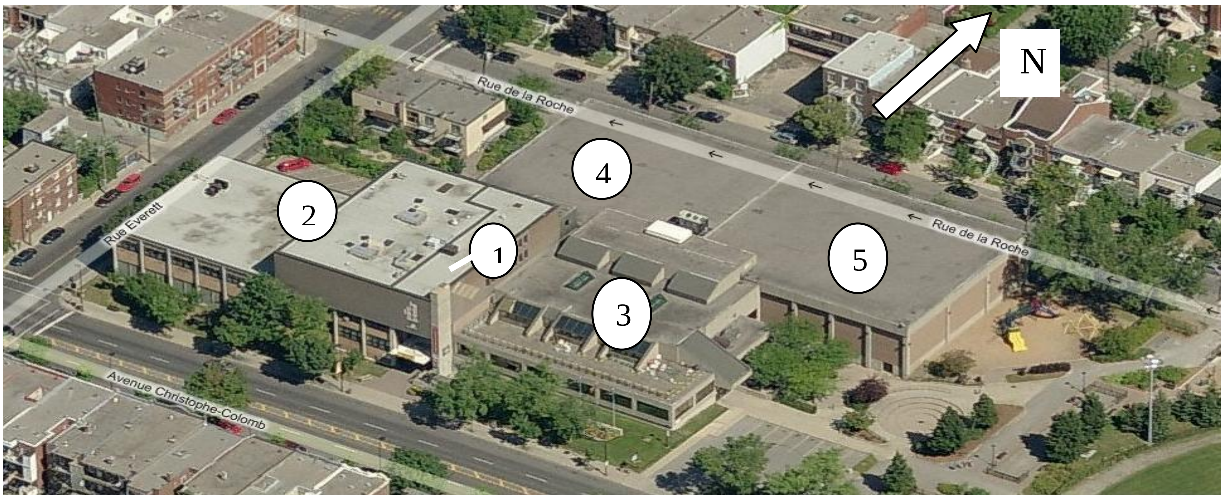


**Figure 3.1.** Complex A - *Patro Le Prévost*'s Bird's eye view

*3.1.1 Building 1*

This building is a six-story reinforced concrete moment frame, which comprises two basements, with total height of 21 m (above the foundation level). The first three floors have a rectangular shape approximately 6.4 m by 32 m, and the upper three stories have an L-shape plan (Fig. 3.1). The position of the sensors used for all test setups combined together is shown in Fig. 3.2: this layout is created in the ARTeMIS software and serves an approximate representation of the building shape. The blue arrows in the figure are the two reference sensors (also marked with R) and the rest (shown in green color) are roving sensors. AVT results with these sensors have allowed the extraction of the first three modes shapes of the building, illustrated in Fig. 3.3.

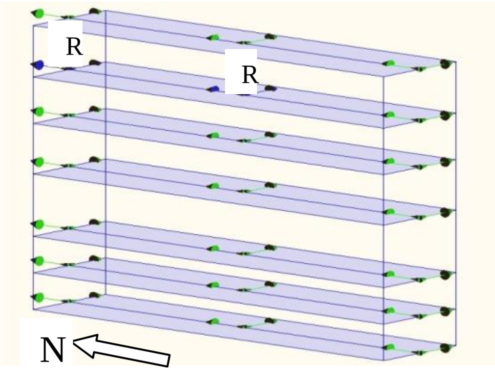


**Figure 3.2.** Sensor positions of all test set-ups - Complex A Building 1

a) b) c)

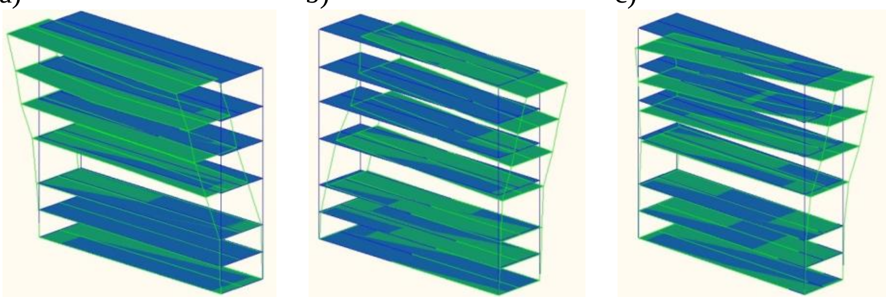

**Figure 3.3.** Mode shapes of Complex A Building 1: a) 1st flexural-torsional mode (3.33Hz); b) 2nd flexural-torsional mode (4.52 Hz); c) 1st torsional mode (5.47 Hz)

*3.1.2 Building 2*

This building is a five stories irregular reinforced concrete moment frame with the total height of 21 m. The bottom floors are rectangular, approximately 32 m by 46 m, respectively; however, the two upper floors have smaller dimensions of approximately 19 m by 32 m, respectively. The sensor positions for all test setups combined are shown in Fig. 3.4, and once again the three lowest frequency mode shapes were extracted from the records and are illustrated in Fig. 3.5.

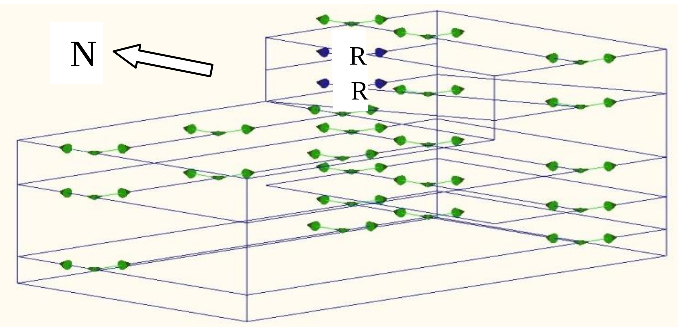


**Figure 3.4.** Sensor positions of all test set-ups - Complex A Building 2

a) b) c)

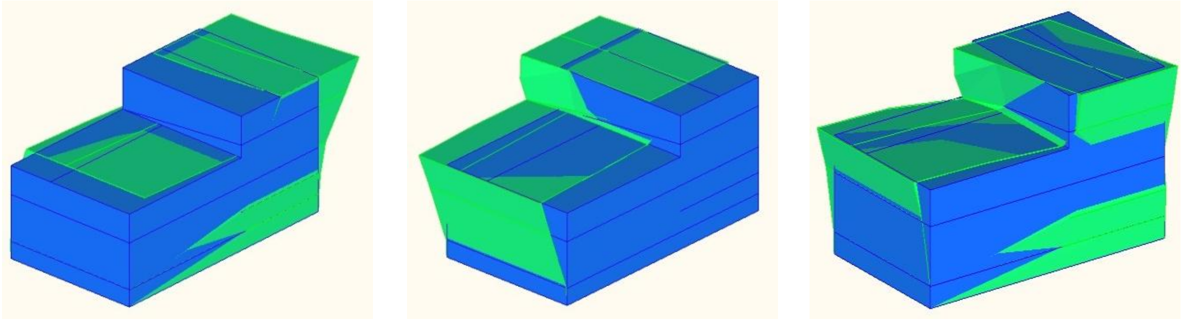

**Figure 3.5.** Mode shapes of Complex A Building 2: a) 1st flexural-torsional mode (3.38 Hz); b) 2nd flexural-torsional mode (4.56 Hz); c) 1st torsional mode (5.47 Hz)

Due to space limitations, not all tested buildings could be described in details here. The remainders three are *Patro Le Prévost*–Building 3, a concrete moment frame with approximate dimensions of 32m by 32 m and 14 m height, and Buildings 4 and 5, two similar two stories steel moment frame buildings of approximate dimensions of 31 m by 37 m and total height of 13 m, including the basement floor.

### 3.2 Complex B: *Centre Pierre-Charbonneau*

This complex is shown in Fig. 3.6 and comprises three joint-separated buildings constructed in 1957. All three buildings are made of reinforced concrete moment frames. Building 1 has a rectangular plan with approximate dimensions of 20 m by 58 m for the ground floor. It has three stories (the first story is a basement) with a total height of 15 m. Building 2 has a rectangular plan with approximate dimensions of 11 m by 52 m for the ground floor: it has three stories with a total height of 11 m. Building 3 is a large single-storey gymnasium with a rectangular plan of 52 m by 58 m.

The sensor positions and the three lowest frequency mode shapes extracted from AVT are shown in Fig. 3.7 and Fig. 3.8, respectively.

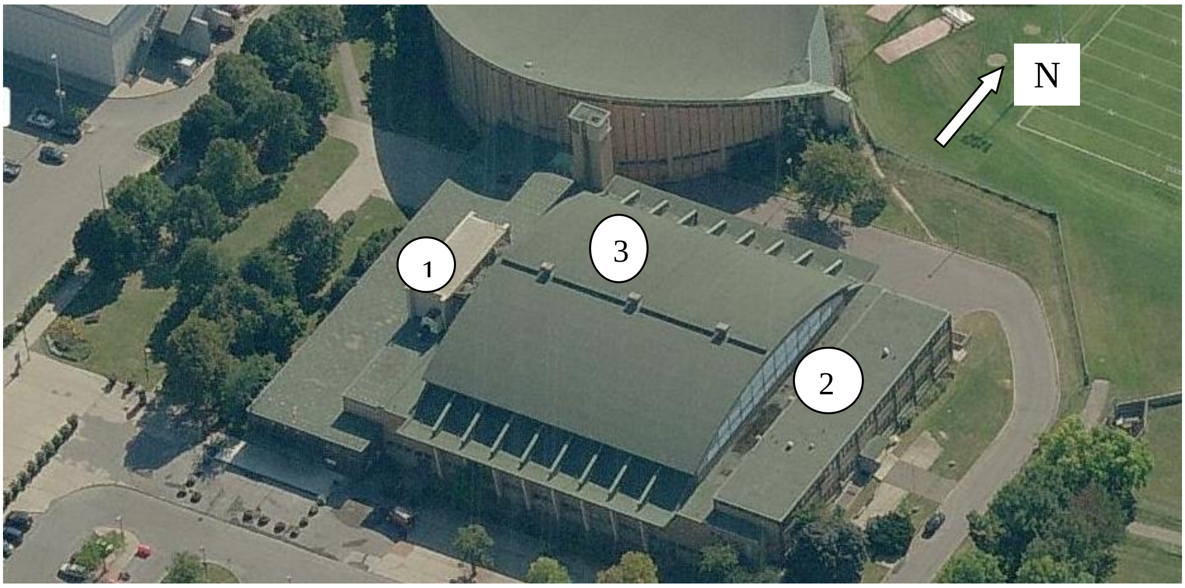


**Figure 3.6.** Complex B - *Centre Pierre-Charbonneau's* Bird's eye view

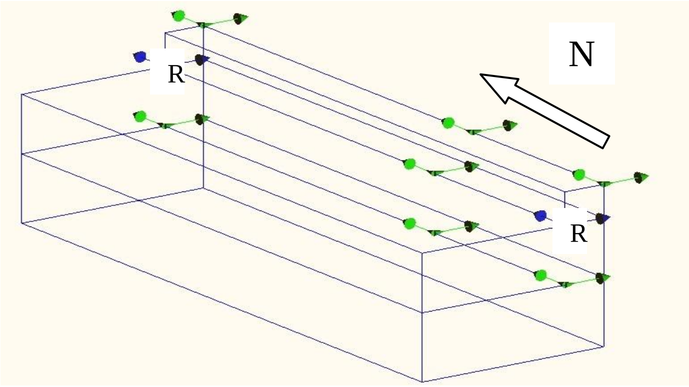


**Figure 3.7.** Sensor positions of all test set-ups – Complex B – Building 1

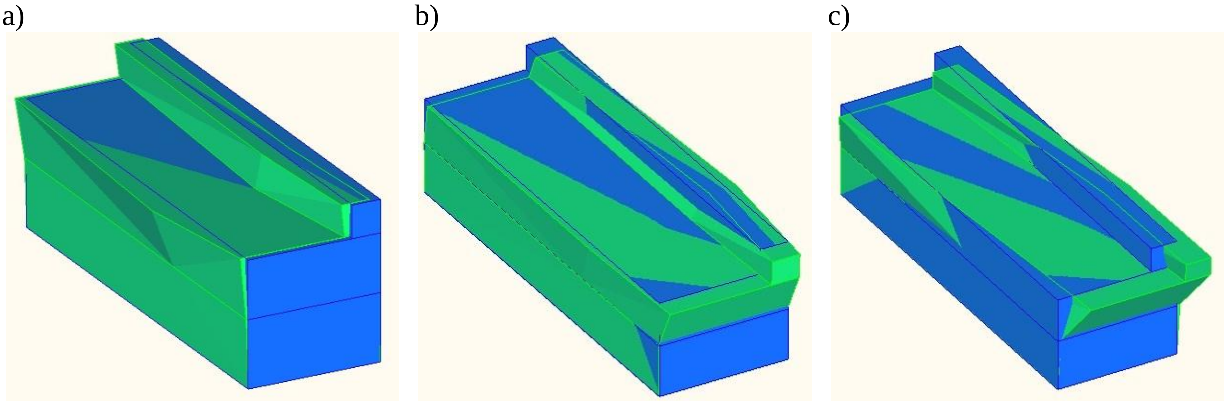


**Figure 3.8.** Mode shapes of Complex B - Building 1 1: a) 1st flexural-torsional mode (6.75 Hz); b) 2nd flexural-torsional mode (8.61 Hz); c) 1st torsional mode (9.95 Hz)

### 3.3 Complex C : *Centre Communautaire de Loisirs de la Côte-des-Neiges*

This complex shown in Fig. 3.9 is a single building constructed in 1993 with a steel braced frame structural system. It has a typical plan of 30 m by 42 m and a total height of 20 m including one basement floor. The sensor positions and the three lowest frequency mode shapes extracted from AVT are shown in Fig. 3.10 and Fig. 3.11, respectively.

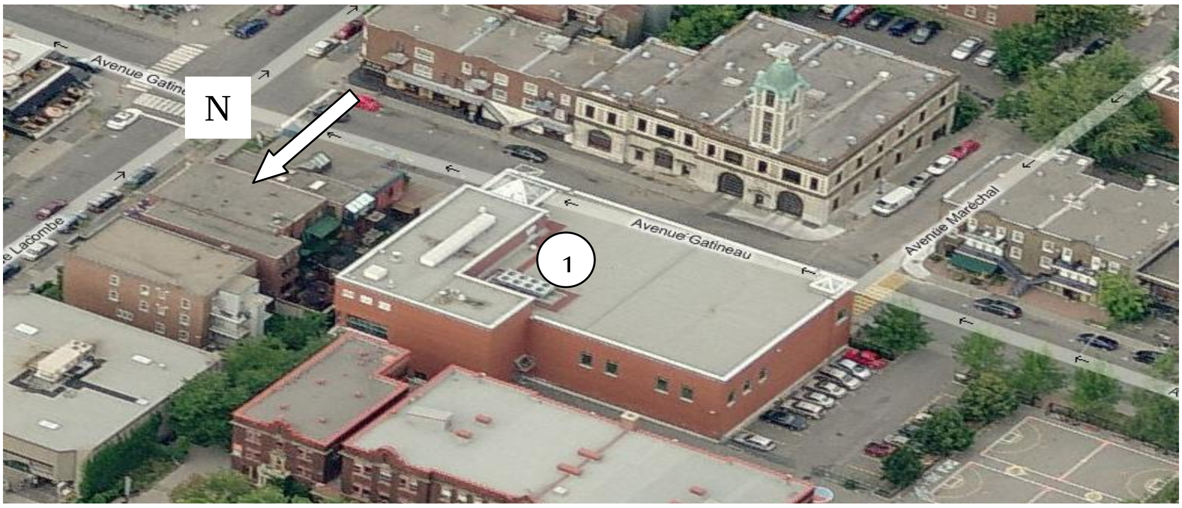


**Figure 3.9.** Complex C - *Centre Communautaire de Loisirs de la Côte-des-Neiges* Bird’s eye view

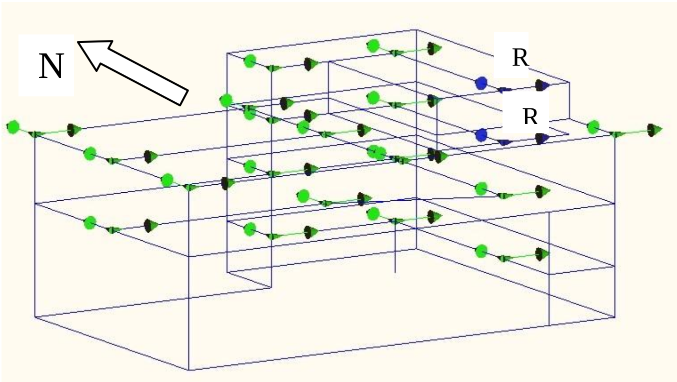


**Figure 3.10.** Sensor positions of all test setups – Complex C

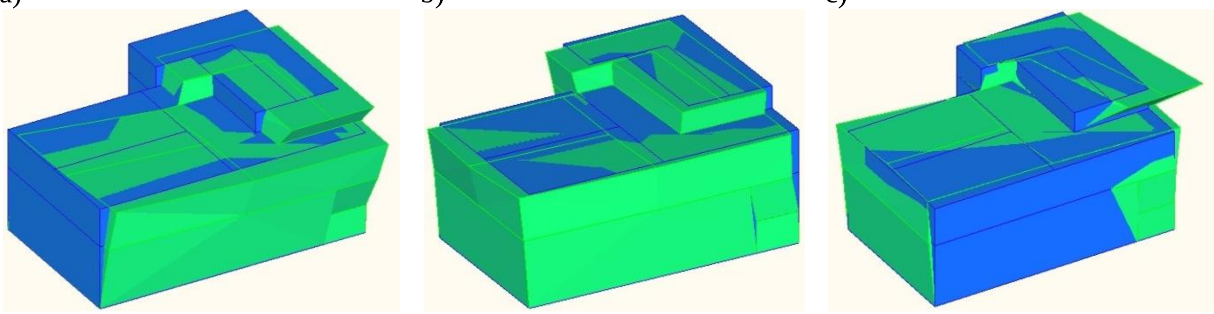


**Figure 11.** Mode shapes of Complex C : *Centre Communautaire de Loisirs de la Côte-des-Neiges:* a) 1st flexural-torsional mode (4.13 Hz); b) 2nd flexural-torsional mode (4.19 Hz); c) 1st torsional mode (5.67 Hz)

## 4. NATURAL FREQUENCIES AND MODAL DAMPING RATIOS

The values of the three lowest natural frequencies and corresponding modal damping ratios corresponding to emergency shelters illustrated in Section 3 are summarized in Table 1. The frequencies are chosen from the best result obtained from FDD and EFDD according to their mode shape configurations. The damping ratio estimates are only available from EFDD, using the logarithmic decrement of the autocorrelation function obtained from the translation of the Spectral Bell function in the time domain. For some cases, the damping ratio or frequency of the third mode could not be identified and the entry NA is shown in the table.

**Table 4.1.** AVT estimated natural frequencies and modal damping ratios for the first three modes

| Building | First mode | | Second mode | | Third mode | |
|---|---|---|---|---|---|---|
| | Frequency (Hz) | Damping (%) | Frequency (Hz) | Damping (%) | Frequency (Hz) | Damping (%) |
| Complex A-Bldg 1 | 3.33 | 2.3 | 4.52 | 2.9 | 5.47 | 2.6 |
| Complex A-Bldg 2 | 3.38 | 2 | 4.56 | 2.3 | 5.47 | 1.6 |
| Complex A-Bldg 3 | 6.69 | NA | 7.78 | NA | 9.45 | NA |
| Complex A-Bldg 4 | 3.73 | 2.5 | 5.44 | 2.3 | NA | NA |
| Complex A-Bldg 5 | 3.31 | 3.2 | 5.23 | 1.5 | NA | NA |
| Complex B-Bldg 1 | 6.75 | 2.9 | 8.61 | 1.4 | 9.95 | 2.4 |
| Complex B-Bldg 2 | 5.42 | 1.5 | 5.69 | 1.3 | 9.99 | 2 |
| Complex B-Bldg 3 | NA | NA | NA | NA | NA | NA |
| Complex C | 4.13 | 1.6 | 4.19 | 1.2 | 5.67 | 2.3 |

It is seen in the table that it was not possible to identify any of the fundamental frequencies of Building 3 of Complex B *Centre Pierre-Charbonneau*: this single story building is a large gymnasium with a curved roof and access to the roof to install sensors was not granted. Otherwise, the frequencies of at least the first two modes could be identified like the other eight buildings.

The coupled flexural-torsional mode shapes obtained for most buildings confirm that these buildings are characterized by structural irregularities. Such irregularities (vertical and horizontal) are usually obvious from the building topologies, but even buildings shape that look symmetric in geometric have eccentricities between their center of mass and center of rigidity at different floor levels.. However, the general trend in the results is that despite the coupling, the first two modes are mainly translational, while the third is torsional. Also, the approximate modal damping values extracted from the results are all below 3.2% viscous critical.

## 5. CONCLUSION

This paper has presented partial results of an on-going research project on field of assessment of low-rise irregular buildings. These results show the feasibility of AVT and structural identification for low and mid-rise irregular buildings. Coupled sway and torsional mode shapes expected to exist in these types of buildings are indeed identified. These test results are part of a larger database that will be used to validate a simplified procedure based on experimental structural parameters to assess the seismic vulnerability of irregular buildings.


### AKCNOWLEDGEMENTS

This work was funded by the McGill Faculty of Engineering doctoral award program (MEDA) and the Natural Sciences and Engineering Research Council (NSERC) of Canada through the Strategic Grant Program and the Strategic Networks program through the Canadian Seismic Research Network.


### REFERENCES


Brincker, R., Ventura, C.E and Andersen, P. (2001). Damping estimation by frequency domain decomposition. *19th International conference on Modal Analysis.* Kissimmee, Florida, 5-8 February, P: 698-703.

Brincker, R., Zhang, L. and Andersen, P. (2001). Modal identification of output-only systems using frequency domain decomposition. *Smart Materials and Structures* **10**: 441-445.

Gentile, C. and Gallino, N. (2008). Ambient vibration testing and structural evaluation of an historic suspension footbridge. *Advances in Engineering Software* **39:4**, 356-366.

Gilles, D. (2011). In situ dynamic characteristics of reinforced shear wall buildings. Ph.D thesis. Department of Civil Engineering and Applied Mechanics. McGill University, Montreal, Canada.

Hans, S., Boutin, C., Ibraim, E. and Roussillon, P. (2005). In situ experiments and seismic analysis of existing buildings. Part I: experimental investigations. *Earthquake Engineering & Structural Dynamics* **34:12**, 1513-1529.

Lamarche, C.P., Proulx, J., Paultre, P., Turek, M., Ventura, C.E., Le, T.P. and Lévesque, C. (2009). Toward a better understanding of the dynamic characteristics of single-storey braced steel frame buildings in Canada. *Canadian Journal of Civil Engineering* **36:6**, 969-979.

Lamarche, C.P., Paultre, P., Proulx, J. And Mousseau, S. (2008). Assessment of the frequency domain decomposition technique by forced vibration tests of a full scale structure. *Earthquake Engineering & Structural Dynamics* **3:73**, 487-494.

Michel, C., Guéguen, P. and Bard, P.Y. (2008). Dynamic parameters of structures extracted from ambient vibration measurements: An aid for the seismic vulnerability assessment of existing buildings in moderate seismic hazard regions. *Soil Dynamics and Earthquake Engineering* **28:8**, 593-604.

Tremblay, R., Lamarche, C.P. and Rogers, C.A. (2008). Periods of vibration of a low rise building with a flexible steel deck diaphragm. *Fifth international conference on thin-walled structures*. Brisbane, Australia, 18-20 June, 8 p.

Solution, S.V. (2010), ARTeMIS Handy Extractor, Software for Operational Modal Analysis.

Trifunac, M. D. (1972). Comparisons between ambient and forced vibration experiments. *Earthquake Engineering & Structural Dynamics* **1**:**2**, 133-150.

Ventura, C., Brincker, R., Dascotte, E. And Andersen, P. (2001). FEM updating of the heritage court building structure. *International modal analysis conference-XIX*. Kissimmee, Florida, 5-8 February. **Vol I**: 324-330.

Yu, E., Taciroglu, E. and Wallace, J.W. (2007a). Parameter identification of framed structures using an improved finite element model updating method—Part I: formulation and verification. *Earthquake Engineering & Structural Dynamics* **36**:**5**, 619-639.

Yu, E., Taciroglu, E. and Wallace, J.W. (2007b). Parameter identification of framed structures using an improved finite element model updating method—Part II: Application to experimental data. *Earthquake Engineering & Structural Dynamics* **36**:**5**, 641-660.